J Mater Sci: Mater Med (2008) 19:3411–3418
DOI 10.1007/s10856-008-3488-0

Organic–inorganic interaction between hydroxyapatite and gelatin with the aging of gelatin in aqueous phosphoric acid solution

Myung Chul Chang

Received: 19 August 2007 / Accepted: 28 May 2008 / Published online: 18 June 2008

Abstract Hydroxyapatite (HAp)/gelatin (GEL) nanocomposite was prepared by the solution-precipitation process using $Ca(OH)_2$ in water and aqueous solution of H_3PO_4 in GEL. Before the co precipitation process the GEL powders were dissolved in the aqueous phosphoric acid solution for the phosphorylation of GEL molecules. The chemical variation of the phosphorylated GEL macromolecules was investigated by using attenuated total reflection (ATR) measurement. The crystal growth of HAp became bigger with the long-time aging of the GEL molecules in the phosphoric acid solution, and it resulted from the reduction of length scale of the GEL molecules. The degree of the organic–inorganic interaction was decreased because of the degradation of the GEL macromolecules.

1 Introduction

HAp/GEL nanocomposite [1, 2] using biomimetic [3, 4] coprecipitation has been developed as one of biological bone substitutes [5], which are biocompatible, biodegradable, and finally regenerative for new bone. Biomimetic synthesis [6, 7] of inorganic compounds, such as calcium phosphate (Ca-P) and apatite has gained increasing attention over the last few years, and the major goal is to understand the specific interactions and processes that enable nature to form such sophisticated objects as bone [1, 2]. Such a composite would be especially advantageous for application as bone substitute, and hydroxyapatite [HAp] is one of the major constituents of hard tissue. In the development of biomimetic HAp/GEL nanocomposites using the commercial GEL powders there have been several difficulties to be challenged, in which the complexity of the reaction mechanism and the low toughness value may be typically considered. The information about the chemical interaction between GEL and Ca-P minerals has been less known even though a large part of commercial GEL [8, 9] is produced from the calcified tissue, such as cow bone or pigskin. The development of apatite phase in the GEL matrix is complicate [1–3], because the commercial GEL contains variety of protein species and the different stages of degraded products. In the development of HAp/GEL nanocomposite, most of interests [2, 3, 10] are related with the formation reaction of apatite nanocrystals in the GEL matrix and the chemical coordination between the formed apatite crystals and GEL matrices. The formation of HAp/GEL nanocomposite is based on the organic–inorganic chemistry between Ca^{2+} and phosphorylated GEL molecules. The phosphorylated GEL is prepared through the dissolving of GEL powders in aqueous H_3PO_4 solution, and the phosphorylation of GEL molecules is intimately related with the formation reaction of HAp/GEL nanocomposite. The organic–inorganic interaction and morphology development of apatite phase in the GEL matrix are reported with further degradation of the precursor of GEL molecules in the phosphoric acid solution of water.

M. C. Chang (✉)
MDRCBB, School of Dentistry, University of Minnesota, 16-280 Moos Tower, 515 Delaware S. E., Minneapolis, MN 55455-0329, USA
e-mail: chang083@umn.edu; mcchang@kunsan.ac.kr

M. C. Chang
School of Material Science and Chemical Engineering, Kunsan National University, Kunsan 573-701, South Korea

2 Experimental methods

Details of the preparation of the HAp/GEL nanocomposite have been well reported in elsewhere [2]. The precursors used here were $CaCO_3$ (Alkaline analysis grade, Aldrich, USA), H_3PO_4 (AP grade, Aldrich, USA), and Gelatin (Unflavored, Canada). $CaCO_3$ powders were calcined at 1,150°C for 3 h, and the obtained CaO powders were hydrated at 200°C by using DI water to make pure $Ca(OH)_2$. The amount of $Ca(OH)_2$ and H_3PO_4 was calculated to make 10 g of HAp. The slurry for HAp/GEL nanocomposite was prepared by the simultaneous titration method using peristaltic pumps (Masterflex, Cole-Parmer, USA), a water bath (Boekel, USA), and a pH controller (Bukert 8280H, Germany). Homogeneous suspensions of $Ca(OH)_2$ dispersed in 2 l of H_2O and an aqueous H_3PO_4 solution with GEL were gradually added to the reaction vessel through the peristaltic pumps. After the coprecipitation reaction, the total volume became 4 l with pH adjustment. The temperature and pH of reaction solution in vessel were set and maintained at 37°C and 8.0, respectively. Three grams of GEL powders were dissolved in aqueous solution of H_3PO_4 and maintained at 37°C for 2, 7, 12, 24, 36, and 72 h, respectively. The phosphorylated GEL solution was immediately used for the coprecipitation process of the HAp/GEL nanocomposite. According to the above phosphorylation time-schedule, sample names of the prepared HAp/GEL nanocomposite were coded as H1, H2, H3, H4, H5, and H6, respectively. With the phosphorylation time-schedule, a part of mixture solution of GEL and H_3PO_4 was picked up and dried for characterization. The GEL solution became sticky with drying. The sticky liquid was dropped onto the infrared optical crystal for attenuated total reflection (ATR) measurement. The infrared absorption spectra of samples were measured by a microscopic FT-IR (Magna 750R, Nicolet, USA). The measurements were conducted by transmittance method. The phosphorylated GEL samples were coded as GEL1, GEL2, GEL3, GEL4, GEL5, and GEL6, respectively. As a reference GEL sample for FT-IR analysis, GEL powders were dissolved in water. The swelled gel was coated on the crystal surface and dried at room temperature for ATR measurement. The reference GEL sample was named as GEL0. After the coprecipitation process, the obtained slurries in the solution were aged at 37°C for 24 h. A part of slurries was collected after aging, and microstructure for the slurries was characterized by transmission electron microscopy [TEM; (JEM-1210, JEOL, Japan)]. Microstructures and phases of the dry sample were characterized using scanning electron microscopy [SEM; (JSM-6700F, JEOL, Japan)] and XRD (Siemens 5005), respectively. A chemical interaction between Ca-P and GEL macromolecules was estimated using the diffuse reflectance FT-IR (Magna 750R, Nicolet, USA). Following initial analysis of the raw spectra to determine the precise constituents, the spectral band positions were analyzed by using GRAMS AI(7.0) (Thermo Galactic, Salem, USA).

3 Result and discussion

3.1 XRD

The development of HAp (JCPDS card 9-432) crystals in the GEL matrix was confirmed from XRD (Fig. 1a, b). From (211) and (201) peaks the samples show the typical crystal development of HAp/GEL nanocomposite [2]. In Fig. 1a H1, H2, and H3 show the broad diffraction peaks, indicating the existence of nanocrystalline phase. In the range of aging time between 2 and 12 h, the (211) and (112) peaks became more diffusive and weaker with the increase of aging time, indicating the formation of nanocrystallites. In Fig. 1b, the 24 h aging sample of H4 shows the diffraction pattern similar with that of H3 in Fig. 1a. For the preparation of HAp/GEL nanocomposite [1–3, 10], we have treated the GEL in aqueous H_3PO_4 solution between 12 and 24 h. In H5, and H6 the (211) peak became less diffusive, indicating the crystal growth.

We have set up the pH as 8.0 to precipitate the HAp phase in GEL matrix [1–4]. The formation of Ca-P phase depends on the pH, and various Ca-P phases are formed under the acidic pH range [11–13]. During the coprecipitation reaction between Ca^{2+} and H_3PO_4, the dynamic supply of ionic precursors sensitively affected the local reaction in the reactor. The droplets of Ca^{2+} and H_3PO_4 precursors were mixed, and it was the initiation of the actual ionic reaction to form Ca-P phase in a reactor environment. The amount of the droplets was automatically controlled to keep the pH close to 8, and the solution was well stirred to make a uniform solution. This process is based on a solid-solid phase transition [14, 15] between octacalcium phosphate [OCP] and HAp, which was at the conditions of pH 7.4–8.4 and $[Ca^{2+}] = 0.04–1.0$ mol/l.

3.2 FT-IR

Figure 2a shows the chemical bond formation between GEL and H_3PO_4 with the aging time. The reference sample, GEL0 shows typical amide bands in gelatin [2, 8], such as amide A at 3,312 cm^{-1}, amide B, amide I at 1,642 cm^{-1}, and amide II at 1,542 cm^{-1}. In the aged GEL samples, the amide bands in gelatin were modified and PO_4 bands were developed. Amide A mode at 3,312 cm^{-1} was blue-shifted to 3,370 cm^{-1}. Amide I and II mode appeared between 1,700 and 1,500 cm^{-1}. From Fig. 2b the spectral feature of amide I and II was moderately changed with the

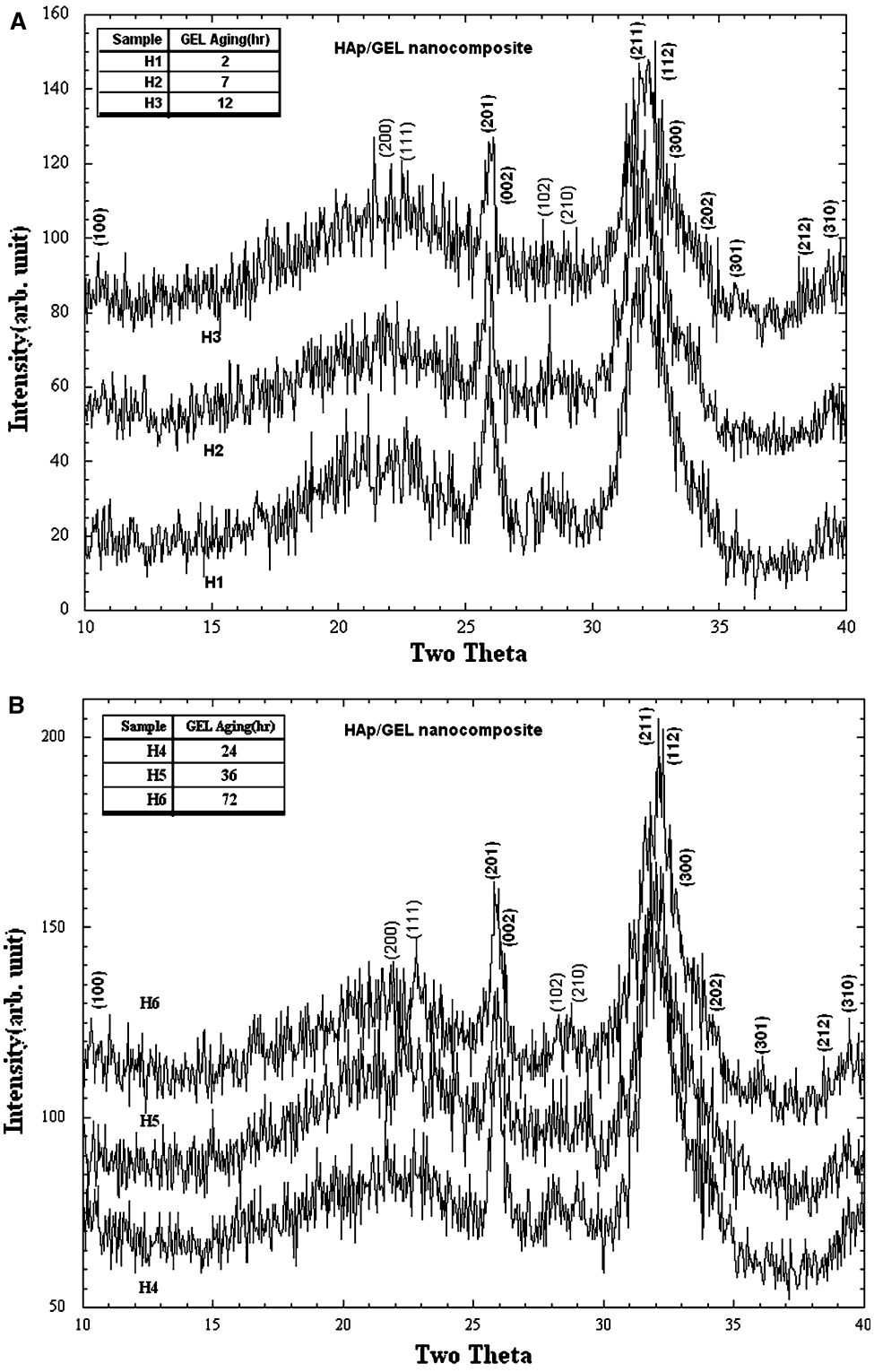

Fig. 1 XRD patterns (**a**) for H1, H2 and H3, and (**b**) for H4, H5 and H6

aging between GEL1 and GEL4. In GEL5, and GEL6 the spectral feature was considerably changed. Band frequencies of amide I and amide II were little shifted. In Fig. 2a the 1,339 cm^{-1} band corresponds to the wagging vibration mode in proline side chains of GEL molecules. The wagging vibration band is red-shifted to 1,335 cm^{-1} through the chemical bond formation of carboxyl ions with Ca^{2+} in HAp nanocrystals [2]. In this preparation condition at pH 8, the carboxylic groups of GEL are largely ionic in the form and offer binding sites for Ca^{2+} ions because of ionic attraction [16]. As can be seen in Fig. 2a, the aged GEL samples show the strong phosphate band between 1,200

and 850 cm^{-1}. The PO_4 spectral feature supports the characteristic information for the phosphate ion coupling in the GEL molecules, which were aged in aqueous phosphoric acid solution. In Fig. 2c the band frequency of PO_4 v_3 mode was red-shifted from 1,115 cm^{-1} of GEL1 to 1,111 cm^{-1} of GEL6. Band frequency of PO_4 v_1 was shifted from 964 cm^{-1} of GEL1 to 960 cm^{-1} of GEL6. The band frequencies were considerably shifted in the samples of GEL5 and GEL6.

In FT-IR spectra for HAp/GEL nanocomposite (Fig. 3a), the band frequency of amide A mode was blue-shifted with the phosphorylation of GEL molecules. The band position of amide A is sensitive to the GEL conformation [8, 9]. It is known that the most significant change of GEL, compared to the native collagen spectrum, is the blue-shift (25–30 cm^{-1}) of the amide A band [17]. That is, the high amide A frequency is characteristic of some level of collagen [COL] structure which is lost upon heating. GEL is the water-soluble product of the dissolution, disorganization or degradation of the water-insoluble collagen fibers [8]. The molecular template of GEL was chemically degraded by the introduction of H_3PO_4, and so the limit of length scale was changed. If the GEL reacts with a dilute H_3PO_4 solution, the phosphorylated GEL molecules will be initially formed without the reduction of length scale. That is, the chemical complex of GEL and H_3PO_4 will be formed. However, the long-time aging in H_3PO_4 will induce the chemical degradation of the GEL molecules. The chemical complex can be broken with the long-time aging in H_3PO_4, corresponding to a chemical degradation process of the GEL molecules.

Figure 3b shows the amide I, II, and PO_4 spectra in the range of 1,800–600 cm^{-1} for H1, H4, H6, and HAP samples. HAP is a hydroxyapatite sample, which was precipitated at 37°C without using GEL. The existence of apatite phase has been confirmed from high PO_4 bands (v_1, v_3) [1–4, 10, 11]. The organic coordination of HAp with the GEL matrix is confirmed from amide bands and PO_4 bands

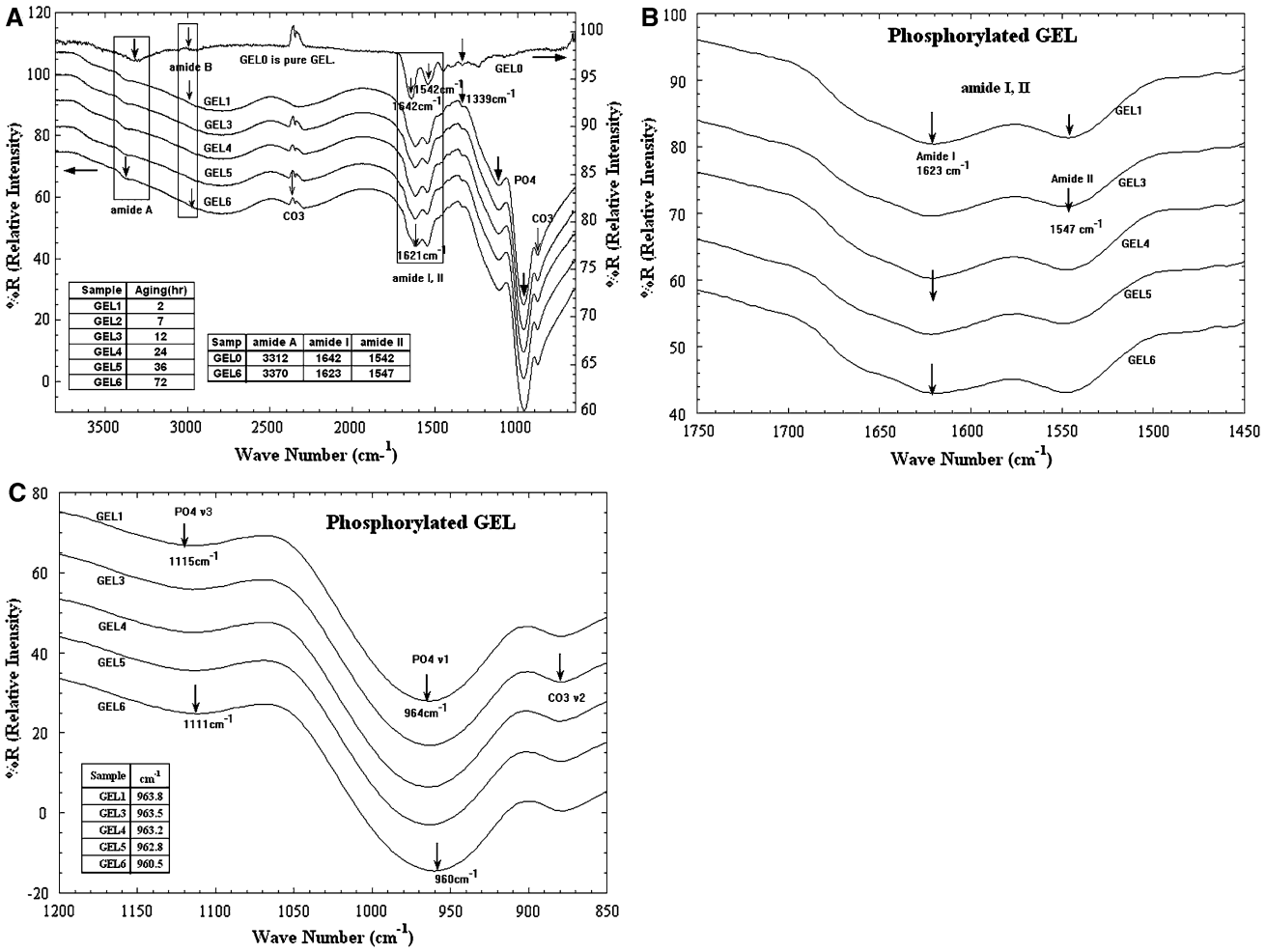

Fig. 2 (**a**) Entire FT-IR spectra for the samples of GEL0, GEL1, GEL3, GEL4, GEL5, and GEL6. GEL0 is a reference GEL sample, prepared without using H_3PO_4. The inner table shows the frequency shift of amide A, I, II band. (**b**) FT-IR spectra for Amide I, II band in the range of 1,450–1,750 cm^{-1}. (**c**) FT-IR spectra for PO_4 v_1, v_3 band in the range of 1,250–850 cm^{-1}

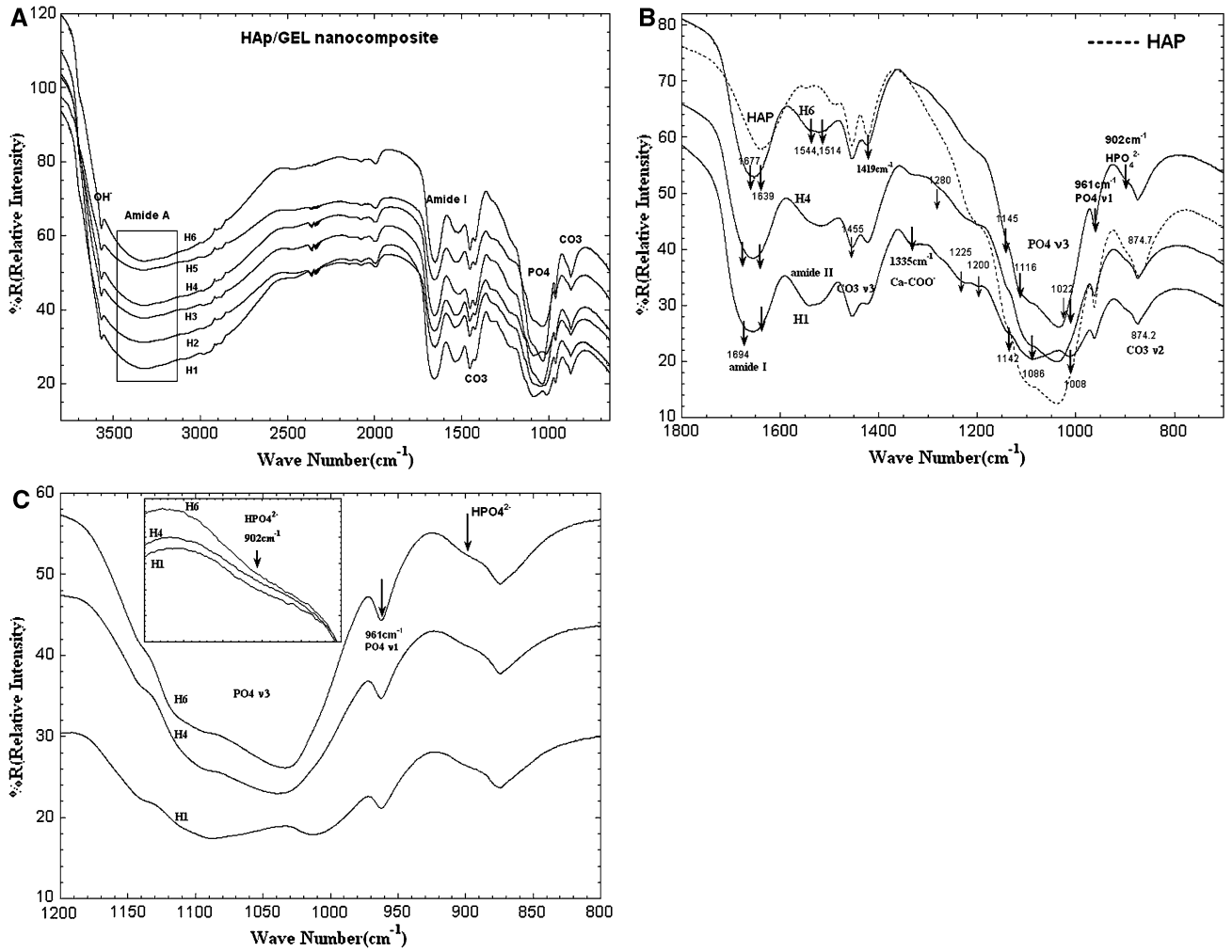

Fig. 3 (**a**) Entire FT-IR spectra for the samples of H1 to H6. (**b**) Amide I, II, III, and PO_4 band spectra for H1, H4, H6, HAP in the range of 1,800–600 cm^{-1}. The Ca^{2+}–COO^- bond spectra at 1,335 cm^{-1} are smeared with the increase of aging time. HAP, dashed line, is a reference HAp sample, prepared without GEL matrix. (**c**) Phosphate contours between 1,200 and 800 cm^{-1}: PO_4 v_1 961 cm^{-1} and HPO_4^{2-} 902 cm^{-1} are getting stronger with the aging

with the aging time. We can observe the typical bands, such as C=O stretching at 1,700–1,600 cm^{-1} for amide I, N–H bending at 1,550–1,500 cm^{-1} for amide II, and N–H deformation at 1,300–1,200 cm^{-1} for amide III band. From the spectral change of the amide I, II, and PO_4 bands, the formed Ca-P phase in H6 was still coordinated with the GEL matrix molecules, indicating the organic–inorganic interaction. It is noted that the spectral behavior of high PO_4 bands (v_1, v_3) in H6 is close to that of HAP. The spectral feature of PO_4 v_3 band approaches to that of HAP with the increase of aging time. The chemical bond formation between the GEL and apatite was weakened with the degradation of the GEL macromolecules in H_3PO_4. The organic–inorganic interaction binding between HAp phase and the GEL matrix could be confirmed from the existence of strong amide bands of amide I and II. From the GRAMS AI analysis for amide I and II band, the band frequencies of the amide I spectra pattern become less diversified and the intensity becomes lower with the aging from H1 to H6. The PO_4 v_3 spectra pattern of H1 is smooth, compared to that of H6. In the HAp/GEL nanocomposite the PO_4 v_3 spectra are smeared if more amount of GEL is bound with Ca-P [2]. So, we can say that the amount of organic–inorganic interaction decreased with the aging of the GEL. As another evidence of the organic–inorganic interaction, the spectral feature of Ca^{2+}–COO^- bond [2] at 1,335 cm^{-1} is smeared with the aging of the GEL.

Figure 3c shows the PO_4 bands in the range of 1,200–800 cm^{-1}. The FT-IR spectral feature of PO_4 v_1 domain at 961 cm^{-1} became stronger with the aging. From the inner diagram we can see that the spectral feature of 902 cm^{-1} band indicating HPO_4^{2-} appeared with the long-time aging. The tetrahedral PO_4 bands of v_1, v_3, show the entire effect of triprotic acid ions in H_3PO_4, but the 902 cm^{-1} band spectra typically show the chemical coordination by HPO_4^{2-} group [11]. From the overall results of Fig. 3 it is considered that

there is a reaction competition between the formation of Ca-P phases and the organic–inorganic interaction with the aging of the GEL molecules. Ca^{2+} can react with aqueous phosphoric acid, phosphorylated group, and/or carboxylic group in the GEL matrix. If we think about HPO_4^{2-} only, the amount at 902 cm^{-1} band increased with the long-aging time in H6. H1 shows a slight amount of HPO_4^{2-}, and H6 shows more amount of HPO_4^{2-}. In H1 sample, the length scale of the GEL macromolecules will be enough stable, and so entire phosphorylated amines will be quickly consumed for a chemical interaction with Ca^{2+}. In the precipitation reaction at pH 8, the most predominant species of phosphoric acid will be HPO_4^{2-} and PO_4^{3-}. However, it is not clear if entire amount of HPO_4^{2-} in H1 and H6 belong to the phosphorylated group of the GEL macromolecules or the free inorganic Pi in the solution. If there is enough amount of free phosphate ion of inorganic Pi, the morphology development in H6 might be affected by the existence of free HPO_4^{2-}. There is a possibility that the HPO_4^{2-} could also be incorporated in the lattice structure of the precipitated apatite. It is a common ion present in non-stoichiometric apatites.

From 1,335 cm^{-1} band spectra (Fig. 3b) indicating the existence of Ca–COO^- complex between HAp and the GEL molecules, most of free Ca^{2+} was consumed during the coprecipitation process. If unreacted side groups in the GEL molecules still exist after the coprecipitation, it will serve for the organic binding among the slurries of HAp/GEL nanocomposite. Water immersion test for the HAp/GEL nanocomposite sample was performed for several months. We could confirm that a small amount of free GEL was released.

3.3 TEM and SEM

From TEM morphology for H2 in Fig. 4a the dilute mineralization of the GEL molecules could be observed. In H6,

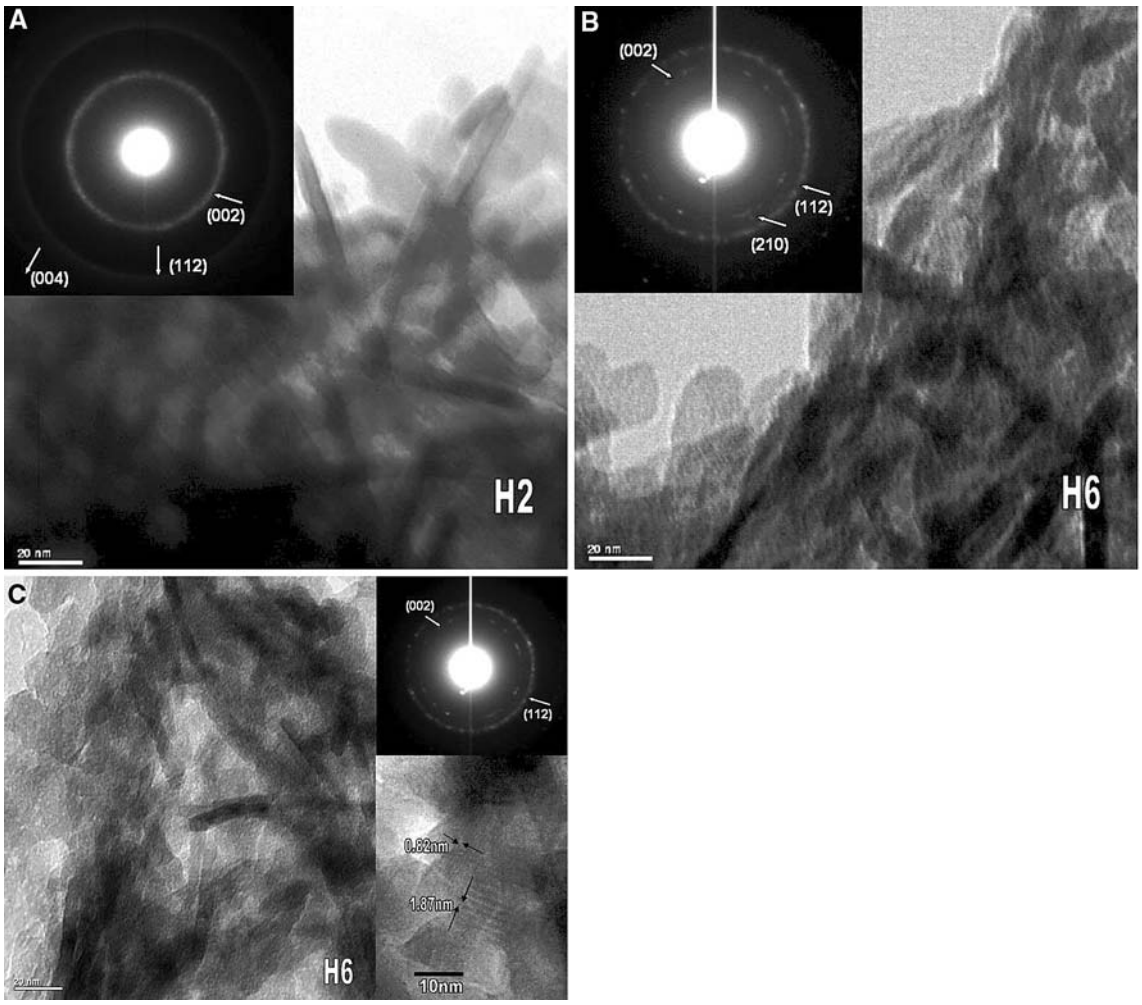

Fig. 4 TEM morphology and ED, showing needle-shaped particles of HAp phase for a mineralization contour. (**a**) HAp phase for H2, (**b**) for H6 and (**c**) for H6. HAp phase with OCP for H6. Lattice image of OCP could be often found during the higher magnification observation for H6 sample

the length scale of the GEL macromolecules will be smaller than that of H2, and so free Ca^{2+} can directly interact with phosphorylated amines and/or phosphoric acid in water. If the length scale is sufficiently big, there are enough amine sites for the chemical bonding with the phosphoric acid. In this case, most of triprotic acids may be instantly consumed for the phosphorylation of GEL. If the GEL is degraded by phosphoric acid, the length scale will be shortened. Moreover, the side groups of GEL molecules may be broken by the chemical degradation. There will be free phosphoric acid, depleted from the phosphorylated GEL. The organic–inorganic interaction between GEL template units and HAp nuclei will occur in the much smaller region. The precipitation reaction will be very fast in the local region, and the crystal size in HAp/GEL composite will be increased. The chance of precipitation for the calcium ion will be limited because there are no more carboxyl sites left in the GEL template. The calcium ion will be attached on the crystal surface in the HAp/GEL nanocomposite, and so the crystal will be grown. In H6, PO_4^{3-} in the GEL will mostly interact with Ca^{2+}, because the phosphoric acid was fully dissociated and the GEL was sufficiently phosphorylated for 72 h. The phosphorylated GEL molecules having small length scales will be completely consumed through the interaction with Ca^{2+}, and so the inorganic Ca-P phase without organic coordination may be formed.

Figure 4 shows TEM micrographs with ED for H2 and H6. It is a typical micrograph for HAp/GEL nanocomposite [2, 3]. From the clear ring patterns it is certain that the mineralization of GEL macromolecules well occurred. The ED pattern for H2 (Fig. 4a) shows the small spots and diffused ring pattern, indicating the existence of nanocrystalline phase. The SAED pattern was indexed by using HAp (JCPDS card 9-432). It seems that the concentration of HAp phase per each GEL molecule template was low, and the composite slurries were overlapped. This might induce the diffused ring spots (Fig. 4a). During TEM observation for H6, OCP lattices ($Ca_8H_2(PO_4)_6 \cdot 5H_2O$, JCPDS 26–1056) could be occasionally detected [12] with HAp as a main phase (Fig. 4b, c). The detected lattice image was varied with the observation time, and some of the observed lattice images disappeared by the impact of strong electron beam injection. Therefore, the lattice image (Fig. 4c) for H6 was transiently obtained. The SAED ring pattern of H6 shows the clearly distinct spots, which are stronger than that of H2.

Figure 5 shows SEM micrograph indicating the dense microstructure. The right-side views are the magnified pictures for each rectangle area. In H2 the magnified image shows a regularly arranged network structure of fine crystallites (Fig. 5a). In H6, the image (Fig. 5b) shows the less uniform structure of bigger crystallites. From Fig. 4 the dimension of needle particles can be approximately

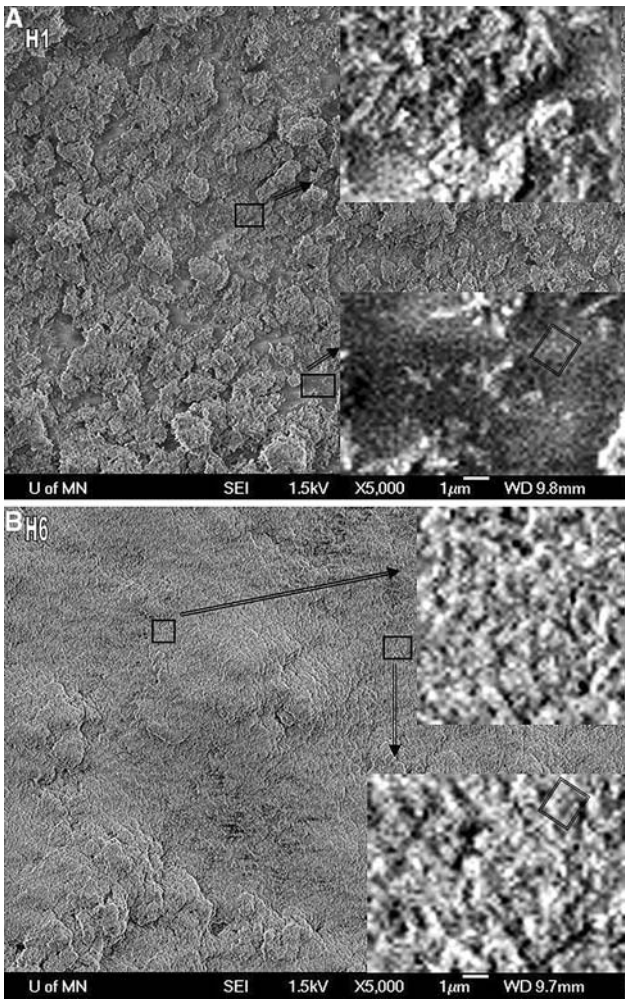

Fig. 5 SEM micrographs for H2 (**a**) and H6 (**b**). The arrowed right-side views are the magnified pictures for each rectangle. (**a**) H2 shows a dense microstructure for more organized composite of HAp/GEL. The composite layers are uniformly overlapped. (**b**) H6 shows the less organized structure because of bigger crystallites of HAp. The square region, noted by a double rectangle, represents a periodic array of nanocomposite particles having several 10 nm diameter

estimated as 5–7 nm in width and 50–100 nm in length. Diameter of small particles shown in Fig. 5 can be estimated as $\sim$0.02 μm. That is, a particle having $\sim$20 nm diameter in Fig. 5 is the agglomerates of needle particles ($\sim$5 nm W $\times$ $\sim$100 nm L), which are shown in Fig. 4. It means that about hundred needle particles of HAp/GEL nanocomposite were conglomerated. The particles were periodically arrayed and overlapped as shown in the magnified SEM view of Fig. 5.

4 Conclusion

Mineralization of the GEL macromolecules was sensitively affected by the phosphorylation of the GEL precursor. The

degradation of phosphorylated GEL caused the reduction of length scale of GEL molecules as a template for the mineralization. Long-time aging more than 24 h contributed to the crystal growth of HAp in the GEL matrix through the degradation of GEL template.

References

1. M.C. Chang, W.H. Douglas, J. Tanaka, J. Mater. Sci. Mater. Med. **17**, 387 (2006)
2. M.C. Chang, C.-C. Ko, W.H. Douglas, Biomaterials **24**, 2853 (2003)
3. M.C. Chang, C.-C. Ko, W.H. Douglas, Biomaterials **24**, 3087 (2003)
4. M.C. Chang, T. Ikoma, M. Kikuchi, J. Tanaka, J. Mater. Sci. Mater. Med. **13**, 993 (2002)
5. R.A. Young, Clin. Orthopedics **113**, 249 (1975)
6. S. Mann, G.A. Ozin, Nature **365**, 499 (1996)
7. E. Dujardin, S. Mann, Adv. Eng. Mater. **4**(7), 461 (2002)
8. A. Veis, *The Macromolecular Chemistry of Gelatin* (Academic Press, London, 1964)
9. A.G. Ward, A. Courts, *The Science and Technology of Gelatin* (Academic Press, London, 1977)
10. M.C. Chang, W.H. Douglas, J. Mater. Sci. Mater. Med. **18**, 2045 (2007)
11. R.Z. Legeros, *Monogr. Oral. Sci. Vol. 15, Calcium Phosphates in Oral Biology and Medicine* (Kager, Basel, 1998), p. 1
12. M. Iijima, *Monogr. Oral. Sci. Vol. 18, Octacalcium Phosphate, Formation of Octacalcium Phosphate In Vitro* (Kager, Basel, 1998), pp. 16–49
13. L.C. Chow, J. Ceram. Soc. Jpn. **99**, 954 (1991)
14. A.L. Boskey, A.S. Posner, J. Phys. Chem. **80**, 40 (1976)
15. W.P. Inskee, J.C. Silvertooth, Geochim. Chosmochim. Acta **52**, 1883 (1988)
16. R.J. Jakobsen, L.L. Brown, T.B. Hutson, D.J. Fink, A. Veis, Science **220**, 1288 (1983)
17. E.P. Paschalis, E. Dicarlo, E. Betts, P. Shermann, R. Mendelsohn, A.L. Boskey, Calcif. Tissue Int. **59**, 480 (1996)